Author/s:
Yang, F;Zhang, M;Fang, Z;Liu, Y

Title:
Impact of processing parameters and post-treatment on the shape accuracy of 3D-printed baking dough

Date:
2019-01-01

Citation:
Yang, F., Zhang, M., Fang, Z. & Liu, Y. (2019). Impact of processing parameters and post-treatment on the shape accuracy of 3D-printed baking dough. International Journal of Food Science and Technology, 54 (1), pp.68-74. https://doi.org/10.1111/ijfs.13904.

Persistent Link:
https://hdl.handle.net/11343/284956

PROF. MIN ZHANG (Orcid ID : 0000-0001-8107-5212)

DR. ZHONGXIANG FANG (Orcid ID : 0000-0002-9902-3426)

Article type : Original Manuscript

Impact of processing parameters and post-treatment on the shape accuracy of 3D-printed baking dough

Fan Yang[a], Min Zhang[a,b*], Zhongxiang Fang[c], Yaping Liu [d]

[a]*State Key Laboratory of Food Science and Technology, Jiangnan University, 14122 Wuxi, Jiangsu, China*

[b]*Jiangsu Province Key Laboratory of Advanced Food Manufacturing Equipment and Technology, Jiangnan University, China*

[c]*Faculty of Veterinary and Agricultural Sciences, The University of Melbourne, Parkville, Victoria 3010, Australia*

[d] *Guangdong Galore Food Co. Ltd, Zhongshan 528447, China*

*Corresponding author: Dr. Min Zhang, Professor of School of Food Science and Technology, Jiangnan University, 214122 Wuxi, P. R. China.

Tel.: 0086-510-85877225; Fax: 0086-510-85877225;

E-mail: min@jiangnan.edu.cn

Running Head: Shape accuracy of 3D-printed baking dough

Summary

Apart from the material compositions, processing parameters of a 3D printer also affect the modeling effect of printed samples. This paper presents the influence of processing parameters including filament diameter (2.10, 2.30, 2.50 mm), nozzle movement speed (20, 25, 30 mm/s), nozzle diameter (0.8, 1.5, 2.0 mm) and nozzle height (2.10, 2.40, 2.60 mm), as well as that of post-process fast-cooling (-65 °C; 0, 5, 10 min), on the rheological properties and geometric accuracy of a 3D-printed food construct made of baking dough (BD). Results showed that the printed object whose shape best matched the target geometry could be obtained with the following processing parameters: filament diameter of 2.30 mm, nozzle movement speed of 25 mm/s, nozzle diameter of 2.0 mm, and nozzle height of 2.40 mm during 3D printing, combined with fast-cooling at -65 °C for more than 10 min after printing and before baking.

Keywords 3D printing, processing parameters, post-process fast-cooling, modeling effect, rheological properties.

Introduction

Three-dimensional printing (3DP) is a new technology that uses computer-assisted layer-by-layer deposition of materials to produce 3D objects (Hao *et al.*, 2010). Unique advantages of 3DP include minimal labor and the capacity to manufacture extremely intricate shapes, making it suitable for a wide range of applications, especially in a fast-increasing consumer goods industries such as the food industry (Drury, J. L. & Mooney, D. J., 2003; Galantucci, L., Lavecchia, F. & Percoco, G., 2009; Godoi, F. C., Prakash, S. & Bhandari, B. R., 2016; Li *et al.*, 2015; Tumbleston *et al.*, 2015; Khalil, S. & Sun, W., 2007; Sun *et al.*, 2015； Zoran, A. & Coelho, M., 2011).

The demand of food printing has immense growth potential, as it can produce new foods with easily-customizable recipes and complex shapes (Wegrzyn, T. F., Golding, M. & Archer, R. H., 2012; Yang, F., Zhang, M. & Bhandari, B. R., 2017). The applications of 3DP in food production are fascinating for both the simple production process and the design of nutritional food with innovative textures (Severini, C. & Derossi, A., 2016). In recent years considerable research has focused on the application of 3DP technology, using various food formulations in the design and production of different types of food constructs. For example, bacon fat and transglutaminase were used to enable scallop and turkey meat-puree to be printable and geometrically stable after cooking (Lipton *et al.*, 2010). The possibility of printing cookies that are ready for baking after printing was investigated (Sun *et al.*, 2015). In addition, some groups have explored the possibility of modeling effects of printing parameters on the quality of printed products. For example, a linear relationship between layer height and extrusion rate in 3D chocolate printing was demonstrated (Hao *et al.*, 2010). However, the relationship between different printing parameters was not fully detailed in these previous studies.

Two conditions are primarily responsible for the quality of 3D-printed samples: the extruding capacity and the shape retention (Yang, F. *et al*., 2018). The extruding behavior of 3DP is actually a shear mechanical behavior which relies on rheological properties such as apparent viscosity for non-Newtonian samples, thus, it plays a vital role in the modeling effect when the composition of the printing material is fixed. Apparent viscosity is the shear stress applied to a fluid divided by the shear rate. Low apparent viscosity would lead to the material that is easily extruded but unable to adequately support the shape and structure of the 3D-printed samples, while high apparent viscosity would lead to bad extruding capacity, leading to 3D-printed products with poor printing accuracy and easily broken lines. Therefore, an intermediate apparent viscosity is crucial for a successful 3D-printed product.

Baking dough (BD) for cookies is a good additive manufacturing food material. Preliminary work with different compositions has already optimized the formulation of this 3D printable BD (Yang, F. *et al*., 2018). However, once the optimized formulation of this BD has been found, there are four main processing parameters that affect 3D-printed products: filament diameter (FD), nozzle movement speed (NMS), nozzle diameter (ND) and nozzle height (NH). In practice selection of suitable

processing parameters is crucial for the successful 3DP of a new product (Anitha, R., Arunachalam, S. & Radhakrishnan, P., 2001). In addition, shape retention of the printed products after baking is also very important, as the extruded dough still needs to be baked prior to being eaten. Therefore, post-process fast-cooling (PPFC) has been used in these experiments to enhance the shape retention of printed samples.

This paper aimed to explore different processing parameters, including FD, NMS, ND and NH, as well as that of PPFC on the rheological properties and geometrical accuracy of a new 3D-printed food construct of BD, and to use mathematical modeling to optimize these parameters of food 3DP. This work also explores variance of post-process parameters such as PPFC time, to improve the geometrically stability of BD after baking. As the available literature on 3DP of food products is limited, the present work may provide useful information for future studies in this emerging area.

Materials and methods

Materials

Ingredients

The BD consisted of icing sugar (crystalline sucrose, moisture content 0.2% (g/g, db), Sugarman Corporation, China), butter (moisture content 0.4%, Lactalis Corporation, France), low-gluten flour (moisture content 14%, Wilmar International Limited, Singapore), eggs (moisture content 73%, local market) and distilled water. Distilled water was used for all experimental work. The standard formulation was a mixture of icing sugar, butter, low-gluten flour, eggs, and water at a ratio of 6.6: 6: 48: 10.4: 29, based on weight. This formulation was derived from that of butter cookies (Zhi, 2014), and was optimized in our previous study (Yang, F. *et al*., 2018).

Preparation of the BD

The refrigerated butter was softened at room temperature for 15 min, then mixed thoroughly with icing sugar in a blender (IKA Co., Ltd, Germany), followed by the addition of egg and further blending until the composition was well mixed.

Subsequently, low-gluten flour and distilled water were blended into the mixture, until a homogenous composition was obtained (Zhi, 2014).

3DP

FD is the diameter of the cylindrical line of material extruded by the printer, i.e. the monolayer height. In the printing process, the nozzle moves on the XYZ axis to constantly adjust its position in relation to the platform, and NMS is the speed of nozzle. ND is the diameter of the nozzle. NH is the distance between the nozzle and the printing platform.

To investigate the effect of such processing parameters on the 3DP properties of the BD, three levels of FD, NMS, ND and NH were tested. FD was set at 2.1, 2.3 and 2.5 mm, respectively. NMS was set at 20, 25 and 30 mm/s, respectively. ND was set at 0.8, 1.5 and 2.0 mm, respectively. NH was set at 2.10, 2.40 and 2.60 mm, respectively. Unless otherwise specified, the standard settings of FD, NMS, ND and NH were 2.3 mm, 25 mm/s, 2.0 mm and 2.40 mm, respectively. The experimental temperature and relative humidity were 24.8 °C and 51%, respectively (Anitha, R., Arunachalam, S. & Radhakrishnan, P., 2001).

An extrusion-based 3D printer (PORIMY Co. Ltd, Kunshan, China) was used in this study. Both FD and NMS which are options in the setup of the controlled software Repetier can be adjusted by the Repetier coupled software. In this experiment, if the printed objects could maintain their shape and structure for at least 20 min, they were considered successfully printed.

PPFC and baking

The 3D-printed samples were fast-cooled in an ultra-low temperature refrigerator, -65 °C, for 0, 5, 10 min, to ensure geometric stability. Once fully frozen (except for the ones with 0 min fast-cooling), all products were baked in an oven at 190 °C for 10 min after which they were ready to be eaten (Zhi, 2014).

Determination of samples quality

3D structure analysis

The 3D-printed shapes in this experiment were a mouse and a square frame. The printed products were measured for their length, width and height by using a vernier caliper. In this experiment, the mouse target design had a length of 95.00 mm, a width of 94.00 mm and a height of 35.00 mm, whereas the square frame target design had a length & width of 100.00 mm and a height of 5.50 mm. The best 3D-printed BD was selected by comparing its dimensions to those of the target designs. The less absolute value of the difference between the dimensions of printed products and the ones of target design that the printer makes, the better shape accuracy of printed products we gets. For each processing parameters, samples were printed in triplicate and measured in triplicate.

Rheological property measurements

The rheological properties were characterized using an AG-G2 Rheometer (AG-1000, Co. TA, USA) with a parallel plate (cone diameter 20 mm, angle 0° and gap 2 mm), at 25 °C. For determination of steady shear viscosities, shear rate (SR) was ramped from 0.1 to 100 s^{-1}. SR and apparent viscosity (η) were recorded by RheoWin 4 Data Manager (Rheology Software, Thermo Fisher Scientific, Waltham, MA).

A creep and recovery test was used, with creep strain of 0.1 Pa and recovery strain of 0 Pa. The measure was done by creep test time of 75, 150 and 300 s, followed by recovery time of 150, 300 and 600 s (Moreira, R., Chenlo, F. & Torres, M. D., 2013). Each sample with different formulations was tested in triplicate.

Data analysis

All equations used for data analysis are presented below:

$$PS = \frac{dL}{dt} \quad (1)$$

where PS is the printing speed (mm/s), *dL* is the extruded sample length when printing (mm), and *dt* is the time used for printing (s).

$$SR = \frac{d\mu}{d\gamma} \quad (2)$$

where SR is the rate at which a progressive shearing deformation is applied to certain material, $d\mu$ is the instantaneous printing speed (mm/s) which equals to the PS value, and $d\gamma$ is the diameter of the tube that connects the electric motor and the extruder (mm).

$$Re = \frac{\rho \mu L}{\eta} \quad (3)$$

where Re equals the Reynolds number, ρ is the density (g/mm^3), and L is the diameter of the tube which connects the electric motor and the extruder (mm).

$$PS = \frac{k*1}{FD^2} \quad (4)$$

where k is the rate empirical parameter.

Supposing that the trust caused by the direct-current electrical machine is constant, all the materials are well-proportioned and printable. Thus, the volume of the feeding material is also constant. In theory, the volume of the printing material per second is equal to the volume of the feeding material per second. Consequently, the PS is inversely proportional to the squared FD. Hence, the model equation was obtained, and written as **Equation (5)**.

$$h_c = \frac{Vd}{NMS*ND} \quad (5)$$

where h_c is the theoretical superior NH (mm), V_d is the volume of extruded material per second (extrusion rate, mm/s) (Wang, J. & Shaw, L.L., 2005).

Experimental data were analyzed using the SPSS 20.0 software (IBM, Chicago, IL, USA), using one-way ANOVA and the Duncan test for pair-wise comparisons, to determine significant differences among the means at 95% confidence level (Gunst, R. F., 1998).

Results and discussion

3DP modeling effect

The printed products with the best shape accuracy are those which most closely resemble what they are designed to. **Fig 1** and **Table S1** showed that the shape

accuracy of the printed products varies inversely with the difference between the length, width and height of the printed products and those of the target designs. The best 3D-printed mouse-shaped BD had a length of 94.62 mm, a width of 94.13 mm and a height of 34.67 mm, whereas the best baked 3D-printed square-frame-shaped BD had a length of 100.35 mm, a width of 100.35 mm and a height of 5.27 mm, indicating the closest length, width and height to the ones of the target design.

Fluid behavior of the extruded materials

This extrusion-based 3D printing process is a kind of mechanical shearing process. Regarding the complex mouse design, the use of different processing parameters resulted in different lengths of sample and printing time, as measured by the Repetier software. Therefore, the PS of each product can be calculated by **Equation (1)**.

SR can then be calculated by **Equation (2)**. All the SR in this experiment were between 0.1 and 2 s^{-1}. From **Fig S1**, with the SR between 0.1 and 2 s^{-1}, **Equation (6)** which is a model based on experimental data can be fitted as follows:

$$\eta = 3.1315r^{-0.623}, R^2 = 0.9991 \quad (6)$$

where η equals the apparent viscosity. Therefore, the apparent viscosities of extruded materials, according to the value of the SR, can be calculated by **Equation (6)**. In a previous study, researchers explored the rheological and extrusion behavior of dental porcelain slurries for rapid prototyping applications, and deduced **Equation (6)**, involving optimized NH and the volume of printed material per second (Wang, J. & Shaw, L.L., 2005).

In addition, the fluid behavior could be considered as either laminar flow or not by the Reynolds number. If the Reynolds number was below 2100, the corresponding fluid behavior was laminar flow, which is known as steady flow (Tian, S. & Barigou, M., 2016). Thus, the Reynolds number was calculated by **Equation (4)**. As shown in **Table S2**, the Reynolds numbers for all samples were below 2100, indicating that all fluid behaviors in this experiment were laminar flow.

Effect of variation of FD on the 3D-printed samples

As shown in **Fig 1**, printed products had the most intact shapes when using FD of 2.30 mm. The FD of 2.50 mm gave the second best print resolution. In contrast, the products generated using a FD of 2.10 mm exhibited the most irregular shapes.

This phenomenon could be due to changes in apparent viscosity between different samples. The PS and apparent viscosities of BD with different FD are presented in **Table S2**. They indicate that, in this printing system, the printing material with FD of 2.10 mm had a relatively lower apparent viscosity (2.84 Pa·s) compared with other FD values, which could be problematic for maintaining shape and structure after printing (**Table S1**). However, when FD was increased to 2.50 mm, the apparent viscosity was also higher (3.52 Pa·s), which might be too difficult to be extruded from the printer, causing lower printing accuracy. This explanation is also supported by **Table S1**, where comparing with the best-shaped sample (obtained with a FD of 2.30 mm), the printed sample with a lower FD (2.10 mm) was longer, wider and thinner, while the printed sample with a higher FD (2.50 mm) was shorter, narrower and thicker.

Effect of different NMS on the 3D-printed samples

As shown in **Fig 1**, printed products had the best intact shape when using an NMS of 25.00 mm/s. An NMS of 30.00 mm/s gave the next best printed objects, whereas the product obtained using an NMS of 20 mm/s exhibited the most irregular shape.

This phenomenon could also be due to changes in apparent viscosity among the samples. The PS and apparent viscosities of BD with different NMS were presented in **Table 2S**. As shown in **Table 1S** and **Table 2S**, compared to products printed at the NMS of 25.00 mm/s, which had the best intact shape, products printed at NMS of 20.00 and 30.00 mm/s respectively. Both of these samples had relatively higher apparent viscosities (4.71 Pa·s and 3.88 Pa·s) and lower accuracy of printed samples matching with target designs. Also, when the NMS was relatively higher (30.00 mm/s), the corner parts of the printed products could not be adequately printed, which contributed to poor accuracy of the 3D-printed objects compared with the target design. Additionally, high NMS (30 mm/s) might cause dragging of extruded material by the nozzle which might lead to broken surface of printed samples.

Effect of variation of ND on the 3D-printed samples

The surface smoothness and printing precision of an object are primarily affected by the size of the printer nozzle (Yang, F. *et al.*, 2018). As shown in **Fig 1**, printed

products had the best intact shape with a ND of 2.0 mm, followed by the ND of 1.5 mm, whereas the product obtained using a ND of 0.8 mm exhibited the most irregular shape.

This phenomenon could be due to that relatively higher apparent viscosities occurred at smaller values of ND (0.8 mm and 1.5 mm) (**Table 2S**), which led to the lower printing accuracy.

The PS and apparent viscosities of BD with different ND are presented in **Table 2S**. As shown in **Table 2S**, in this printing system, as the ND is increased, the PS also increased, but the apparent viscosity decreased. The smoothness and dimensional accuracy could be enhanced by a smaller nozzle size, but this would cause an increase the pressure or shear experienced by the material at the nozzle, having a negative influence on extrusion behavior. This would lead to lower geometric accuracy when the printed object matching to the target design. Therefore, in this printing system, both 9.44 Pa·s (0.8 mm FD) and 4.40 Pa·s (1.50 mm FD) apparent viscosities might be too high for extrusion, and 3.17 Pa·s (2.0 mm FD) apparent viscosity might be suitable for extrusion.

Effect of different NH on the 3D-printed samples

Attala (2016) indicated that NH significantly affects the geometric shape of printed samples (Attalla, R., Ling, C. & Selvaganapathy, P., 2016). As shown in **Fig 1**, printed products had the best intact shape at a NH of 2.40 mm, followed by the product obtained using the NH of 2.60 mm, whereas the product obtained using a NH of 2.10 mm exhibited the most irregular shape.

By substituting the PS and FD in the **Equation (5)**, we calculated that k = 93.218, and $V_d = 4k/\pi$ =118.689 mm3/s. And D_n = 2.0 mm and v_n = 25 mm/s, thus h_c = 2.37 mm. In **Fig 1**, the NH which had the best modeling effect was 2.40 mm, which was the closest to 2.37 mm in the NH group. As the NH of 2.60 mm was also relatively closer to the NH of 2.37 mm, the modeling effect of the product obtained using the NH of 2.60 mm was better than that of the product obtained using the NH of 2.10 mm.

When the NH was lower than h_c, the extruded lines were much thicker, thus leading to the geometric inaccuracy of printed products. When the NH was higher than h_c, the feeding BD might not reach the print platform when the nozzle turned to a corner, thus also leading to geometric inaccuracy of the printed products. Therefore, when the NH was very close to h_c, the shape of the printed products should be the

297 closest to the target design. Also, as a result of dough swelling/spreading upon
298 extrusion, the optimum NH should be slightly higher than h_c.

299 In an ideal printing process, under the condition of matched extrusion rate and
300 PS, the NH value was supposed to be the same with the ND value (Wang, J. & Shaw,
301 L.L., 2005). However, due to elasticity of material, expansion of extruded material
302 occurred. Thus monolayer height (FD) of material would be slightly higher than the
303 ND. On the other hand, the NH also should be as low as possible to make sure that the
304 extruded material could be fused with earlier printed layers and have no inaccuracy
305 caused by delayed deposition. Thus the theoretical superior NH (h_c) should be very
306 close to FD. Therefore, the optimized NH was selected to 2.40 mm, which was the
307 closest one to h_c considering allowable error of dough swelling upon extrusion.

308

309 Effect of variation of PPFC time on the 3D-printed samples

310 In general, a high baking temperature would cause a certain level of damage to
311 the shapes and structures of 3D-printed food products. For example, cookie dough
312 which initially lost its shape when baked was printed, thus the cookies were chilled in
313 a freezer following extrusion to ensure geometric stability (Lipton *et al.*, 2010).
314 Preliminary experiments of the dough used in this experiment had been confirmed
315 that -65 °C for greater than 10 min provide the best result. In this experiment, all
316 products were frozen except for the products with PPFC time of 0 min, and then all
317 the samples were baked immediately after PPFC.

318 A creep and recovery test was performed, in which a shear stress was forced
319 upon the material. In a creep recovery experiment a stress is applied for a certain
320 duration and then is removed and the recovery is monitored for another certain
321 duration. Less strain during the test indicates a stronger ability of the material to
322 maintain the shape and structure of the printed products. As shown in **Fig 2** and **Table**
323 **1S**, with increasing PPFC time, the baked products had better shapes and structures
324 matching with the target design. This corresponds to these samples also exhibiting
325 less change during the creep and recovery test (**Fig 2S**). With no PPFC before baking
326 (0 min), the samples were seriously collapsed and could not keep their shapes (**Fig 2**).
327 Thus, if 3D-printed food products are to be produced have desired shapes and
328 structures, they should be fast-cooled to -65°C for more than 10 min.

329

Conclusion

The properties and composition of materials ready for printing are considered as important factors in the 3DP process. These materials should be homogenous and have appropriate flow properties for extrusion as well as can support its structure during and after printing process. Besides physical properties of different composition, the results of process optimization for 3DP confirmed that FD, NMS, ND and NH also affect the shape accuracy of printed samples. It was found that FD (2.30 mm), NMS (25 mm/s), ND (2.0 mm), NH (2.40 mm) were optimal parameters for 3DP BD. PPFC (-65 °C; more than 10 min) after printing and before baking was beneficial to maintain the structure and shape of samples after baking. This corresponded to 3.17 Pa·s apparent viscosity when extruded. Moreover, the success of the 3DP BD provided beneficial guidance for other food material in 3DP.

Acknowledgments

The authors acknowledge the financial support from the China State Key Laboratory of Food Science and Technology Innovation Project (Contract No. SKLF-ZZA-201706), National First-class Discipline Program of Food Science and Technology (No. JUFSTR20180205), Jiangsu Province (China) “Collaborative Innovation Center for Food Safety and Quality Control” Industry Development Program, Jiangsu Province Key Laboratory Project of Advanced Food Manufacturing Equipment and Technology (Contract No. FMZ201803), which have enabled us to carry out this study.

References

Anitha, R., Arunachalam, S., & Radhakrishnan, P. (2001). Critical parameters influencing the quality of prototypes in fused deposition modelling. *Journal of Materials Processing Technology*, **118(1-3)**, 385-388.

Attalla, R., Ling, C. & Selvaganapathy, P. (2016). Fabrication and characterization of gels with integrated channels using 3D printing with microfluidic nozzle for tissue engineering applications. *Biomed Microdevices*, **18(1)**, 17.

Drury, J. L., & Mooney, D. J. (2003). Hydrogels for tissue engineering: scaffold design variables

and applications. *Biomaterials*, **24**, 4337-4351.

Galantucci, L., Lavecchia, F., & Percoco, G. (2009). Experimental study aiming to enhance the surface finish of fused deposition modeled parts. *CIRP Annals-Manufacturing Technology*, **58(1)**, 189-192.

Godoi, F. C., Prakash, S., & Bhandari, B. R. (2016). 3D printing technologies applied for food design: Status and prospects. *Journal of Food Engineering*, **179**, 44-54.

Gunst, R. F. (1998). Applied regression analysis, by norman r. draper; harry smith. , **1998**, 1-99.

Hao, L., Mellor, S., Seaman, O., Henderson, J., Sewell, N., & Sloan, M. (2010). Material characterisation and process development for chocolate additive layer manufacturing. *Virtual and Physical Prototyping*, **5(2)**, 57-64.

Khalil, S., & Sun, W. (2007). Biopolymer deposition for freeform fabrication of hydrogel tissue constructs. *Materials Science & Engineering C*, **27(3)**, 469-478.

Li, J.-N., Liu, K.-G., Gong, S.-L., Zhang, Y.-B., & Liu, P. (2015). Physical properties and microstructures of nanocrystals reinforced ice laser 3D print layer. *Physica E: Low-dimensional Systems and Nanostructures*, **66**, 317-320.

Lipton, J., Arnold, D., Nigl, F., Lopez, N., Dan, C., Norén, N., & Lipson, H. (2010). Multi-material food printing with complex internal structure suitable for conventional post-processing. presented at the Solid Freeform Fabrication Symposium (unpublished).

Moreira, R., Chenlo, F., & Torres, M. D. (2013). Rheology of Gluten-Free Doughs from Blends of Chestnut and Rice Flours. *Food and Bioprocess Technology*, **6**, 1476-1485.

Sun, J., Zhou, W., Huang, D., Fuh, J. Y. H., & Hong, G. S. (2015). An Overview of 3D Printing Technologies for Food Fabrication. *Food and Bioprocess Technology*, **8**, 1605-1615.

Severini, C., Derossi A. & Azzollini, D. (2016). Variables affecting the printability of foods: Preliminary tests on cereal-based products. *Innovative Food Science and Emerging Technologies*, **38**, 281-291

Tian, S., & Barigou, M. (2016). Assessing the potential of using chaotic advection flow for thermal food processing in heating tubes. *Journal of Food Engineering*, **177**, 9-20.

Tumbleston, J. R., Shirvanyants, D., Ermoshkin, N., Janusziewicz, R., Johnson, A. R., Kelly, D., Ermoshkin, A. (2015). Continuous liquid interface production of 3D objects. *Science*, **347(6228)**, 1349-1352.

Wang, J. & Shaw, L.L., (2005). Rheological and extrusion behavior of dental porcelain slurries for rapid prototyping applications. *Materials Science and Engineering: A*, **397**, 314-321.

Wegrzyn, T. F., Golding, M., & Archer, R. H. (2012). Food Layered Manufacture: A new process for constructing solid foods. *Trends in Food Science & Technology*, **27(2)**, 66–72.

Yang, F., Zhang, M., Bhandari, B. R., (2017). Recent development in 3D food printing. *Critical Reviews in Food Science and Nutrition*, **57(14)**, 3145-3153.

Yang, F. Zhang, M., Prakash, S. & Liu, Y. P. (2018). Physical properties of 3D printed baking dough as affected by different compositions. *Innovative Food Science and Emerging Technologies*. http://doi.org/10.1016/j.ifset.2018.01.001.

Zhi, J. (2014). http://www.junzhiblog.com/binggan/1177.html

Zoran, A., & Coelho, M. (2011). Cornucopia: the concept of digital gastronomy. *Leonardo*, **44(5)**, 425-431.

Figure captions:

Fig 1. Representative photos of printed samples with different processing parameters, in different groups: (a) FD; (b) NMS; (c) ND; (d) NH

Fig 2. Representative photos of baked printed samples with different PPFC time before baking

Supplementary information captions:

Fig 1S. Apparent viscosity and SR of samples

Fig 2S. Creep and recovery curve of samples with different PPFC time: (a) 0 min; (b) 5 min; (c) 10 min

Table 1S. 3D structure analysis for the mouse design (FD, NMS, ND and NH group) or the square frame design (PPFC time group)

Table 2S. Printing speeds and apparent viscosities of samples, in different groups: FD; NMS; ND; NH

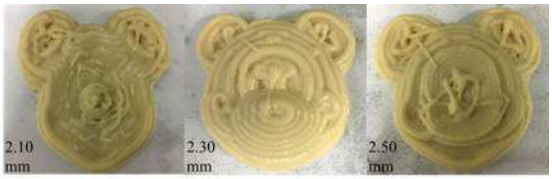

ijfs_13904_f1a.jpg

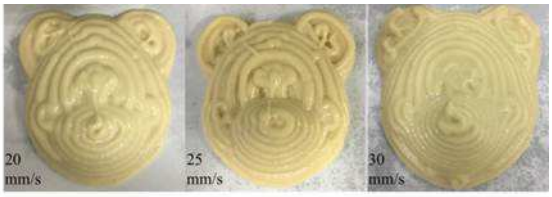

ijfs_13904_f1b.jpg

ijfs_13904_f1c.jpg

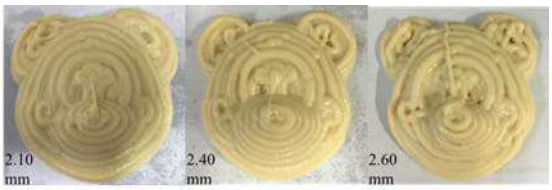

ijfs_13904_f1d.jpg

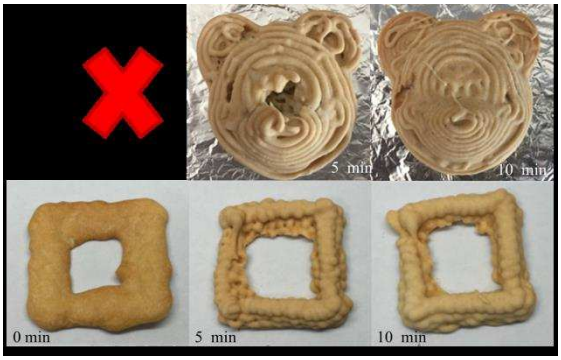

ijfs_13904_f2.jpg